

## RESEARCH ARTICLE

# Conditional *Lpar1* gene targeting identifies cell types mediating neuropathic pain

Richard R. Rivera<sup>1</sup> | Mu-En Lin<sup>2,3</sup> | Emily C. Bornhop<sup>1</sup> | Jerold Chun<sup>1</sup>

<sup>1</sup>Degenerative Disease Program, Sanford Burnham Prebys Medical Discovery Institute, La Jolla, CA, USA

<sup>2</sup>Molecular Biology Department, Dorris Neuroscience Center, The Scripps Research Institute, La Jolla, CA, USA

<sup>3</sup>Biomedical Sciences Graduate Program, University of California San Diego, La Jolla, CA, USA

## Correspondence

Jerold Chun, Degenerative Disease Program, Sanford Burnham Prebys Medical Discovery Institute, 10901 N Torrey Pines Rd, La Jolla, CA 90237, USA.  
Email: jchun@sbbpdiscovery.org

## Present address

Mu-En Lin, RevMAB Biosciences, South San Francisco, CA, USA

## Funding information

HHS | NIH | National Institute of Mental Health (NIMH), Grant/Award Number: R01MH051699; Amira Pharmaceuticals

## Abstract

LPA<sub>1</sub> is one of six known receptors (LPA<sub>1-6</sub>) for lysophosphatidic acid (LPA). Constitutive *Lpar1* null mutant mice have been instrumental in identifying roles for LPA-LPA<sub>1</sub> signaling in neurobiological processes, brain development, and behavior, as well as modeling human neurological diseases like neuropathic pain. Constitutive *Lpar1* null mutant mice are protected from partial sciatic nerve ligation (PSNL)-induced neuropathic pain, however, the cell types that are functionally responsible for mediating this protective effect are unknown. Here, we report the generation of an *Lpar1*<sup>flox/flox</sup> conditional null mutant mouse that allows for cre-mediated conditional deletion, combined with a PSNL pain model. *Lpar1*<sup>flox/flox</sup> mice were crossed with *cre* transgenic lines driven by neural gene promoters for *nestin* (all neural cells), *synapsin* (neurons), or *P0* (Schwann cells). *CD11b-cre* transgenic mice were also used to delete *Lpar1* in microglia. PSNL-initiated pain responses were reduced following cre-mediated *Lpar1* deletion with all three neural promoters as well as the *CD11b* promoter, supporting involvement of Schwann cells, central and/or peripheral neurons, and microglia in mediating pain. Interestingly, rescue responses were nonidentical, implicating distinct roles for *Lpar1*-expressing cell types. Our results with a new *Lpar1* conditional mouse mutant expand an understanding of LPA<sub>1</sub> signaling in the PSNL model of neuropathic pain.

## KEYWORDS

conditional knockout, LPA, PSNL, Schwann cells, neurons

## 1 | INTRODUCTION

Neuropathic pain is produced by nerve lesions or neurological conditions such as multiple sclerosis, diabetes, and cancer and affects an estimated 10% of the general population.<sup>1</sup>

Treatment options for individuals affected by neuropathic pain are limited and ineffective, often leading to a worsened condition and disability. Initiation and propagation of pain signaling occurs through afferent nerve fibers that relay peripheral signals through dorsal root ganglia (DRG) to signal

**Abbreviations:** CNS, central nervous system; DRG, dorsal root ganglia; LPA, lysophosphatidic acid; *Lpar1*, (*LPA receptor 1*); PNS, peripheral nervous system; PSNL, partial sciatic nerve ligation.

Richard R. Rivera and Mu-En Lin contributed equally to this work.

This is an open access article under the terms of the Creative Commons Attribution-NonCommercial-NoDerivs License, which permits use and distribution in any medium, provided the original work is properly cited, the use is non-commercial and no modifications or adaptations are made.

© 2020 The Authors. *The FASEB Journal* published by Wiley Periodicals LLC on behalf of Federation of American Societies for Experimental Biology

via the central nervous system (CNS) spinal cord dorsal horn and brain (reviewed in 2-4). Neuropathic pain involves central sensitization, a process that results in allodynia (painful response to normally innocuous stimuli) and hyperalgesia (increased pain sensation to noxious stimuli).<sup>5</sup>

One identified modulator of neuropathic pain is the bioactive lipid lysophosphatidic acid (LPA). LPA normally signals through six known G protein-coupled receptors, *LPA<sub>1-6</sub>*,<sup>6</sup> which are involved in myriad biological and pathological processes affecting most of the physiological systems in the body, including the nervous system.<sup>6-13</sup> *LPA<sub>1</sub>* is expressed in the peripheral nervous system (PNS) and CNS. Schwann cells represent one of the *LPA<sub>1</sub>* expressing cell types that may be involved in the induction of neuropathic pain. LPA signaling through this receptor influences Schwann cell morphology, migration, and survival.<sup>14,15</sup> In vivo, sciatic nerves of *Lpar1* deficient mice show abnormalities including an increased number of apoptotic Schwann cells, reduced myelin thickness, and a proportionately lower number of small nerve fiber interacting Schwann cells.<sup>14,16</sup> Neurons can also be affected through *LPA<sub>1</sub>*-mediated changes to cell morphology, motility, growth cone collapse, calcium signaling, and proliferation.<sup>16-23</sup> Mice deficient for this receptor display alterations in cortical development and neurogenesis as well as behavioral abnormalities.<sup>22-24</sup>

A role for LPA in pain sensation was first identified through intrathecal (i.t.) injection of LPA, where mice that received a single i.t. injection of LPA developed thermal hyperalgesia and mechanical allodynia.<sup>25</sup> LPA-induced neuropathic pain was accompanied by other sequelae including demyelination in the dorsal root and increased expression of pain associated markers including, protein kinase  $C\gamma$  (PKC $\gamma$ ) in the spinal cord dorsal horn, and voltage-gated calcium channel  $Ca\alpha 2\delta 1$  in the DRG.<sup>25</sup> Interestingly, i.t. injection of LPA also induced de novo production of LPA in the dorsal horn and dorsal root, implicating a feed-forward role in pain generation.<sup>26,27</sup> De novo LPA production was also observed in the dorsal horn and dorsal root following PNL.<sup>28-30</sup> Wildtype (Wt) mice subject to PNL displayed pain behaviors similar to those of mice that received i.t. LPA, and showed similar demyelination as well as upregulation of PKC $\gamma$  and  $Ca\alpha 2\delta 1$ .<sup>25</sup>

LPA's effects in PNL were shown to be receptor-dependent through the use of constitutive null receptor mutants. *Lpar1* null mutant mice were protected from both PNL and i.t. LPA injection induced mechanical allodynia, and did not show accompanying increases of PKC $\gamma$  and  $Ca\alpha 2\delta 1$ .<sup>25</sup> *Lpar5* null mutant mice were also protected from PNL-induced neuropathic pain, albeit through CNS mechanisms distinct from those of *Lpar1* null mutants.<sup>31</sup>

While *Lpar1* null mutant mice are protected from PNL-induced neuropathic pain, the cell types responsible for mediating this protection remain unclear. To address this issue, we generated a *Lpar1* conditional null mutant mouse and targeted deletion of *Lpar1* in all neural lineages, peripheral and

CNS neurons, Schwann cells, and microglia/myeloid cells to identify the cell types responsible for mediating *Lpar1*'s protective effect in the PNL neuropathic pain model.

## 2 | MATERIALS AND METHODS

### 2.1 | Mice

All procedures performed on animals were IACUC approved and performed in accordance with the regulations of The Scripps Research Institute (TSRI) Department of Animal Resources and the Sanford Burnham Prebys Medical Discovery Institute animal care and use committee. Mice used in this study were *nestin-cre* (Jackson Laboratory Stock Number 003 771), *P0-cre* (Jackson Laboratory Stock Number 017 927), *synapsin-cre* (Jackson Laboratory Stock Number 003 966), and *CD11b-cre* (obtained from Don Cleveland) transgenic lines.

### 2.2 | Synthesis of the *Lpar1* conditional gene targeting vector

Creation of the *Lpar1* conditional gene targeting vector was accomplished by PCR amplification of mouse *Lpar1* genomic fragments using a bacterial artificial chromosome (BAC RP23-149020 Children's Hospital Oakland Research Institute (CHORI)) containing the *Lpar1* genomic locus as a template. PCR amplification was performed using *Pfx50* DNA polymerase (Invitrogen) and amplified genomic fragments were assembled into pBluescript II. During the process of assembly, a loxP site was inserted into a HindIII site 5' of *Lpar1* exon 3 and a neomycin cassette under the control of the phosphoglycerate kinase promoter (PGK-neo) flanked by loxP sites was inserted directionally (all loxP sites in the same orientation) into an XbaI site 3' of *Lpar1* exon 3 (Figure 1A). The construct was engineered so that 3.4 and 6.7 kb of *Lpar1* genomic DNA flanked the PGK-neo insertion site. To aid in cloning, BamHI and AatII restriction enzyme sites were added to the distal 5' and 3' ends of the *Lpar1* genomic segment chosen for targeting vector design. An EcoRI restriction enzyme site was included in the loxP flanked PGK-neo cassette to identify ES cell clones containing an allele that recombined homologously with the targeting vector.

### 2.3 | Production of *Lpar1*<sup>lox/lox</sup> and *Lpar1*<sup>lox/lox</sup>-cell type-specific null mutant mice

To create the *Lpar1*<sup>lox/lox</sup> mice,  $1 \times 10^7$  R1 ES cells were mixed with 50  $\mu$ g of linearized *Lpar1* targeting vector in a 0.4 cm electroporation cuvette and the cells were pulsed with

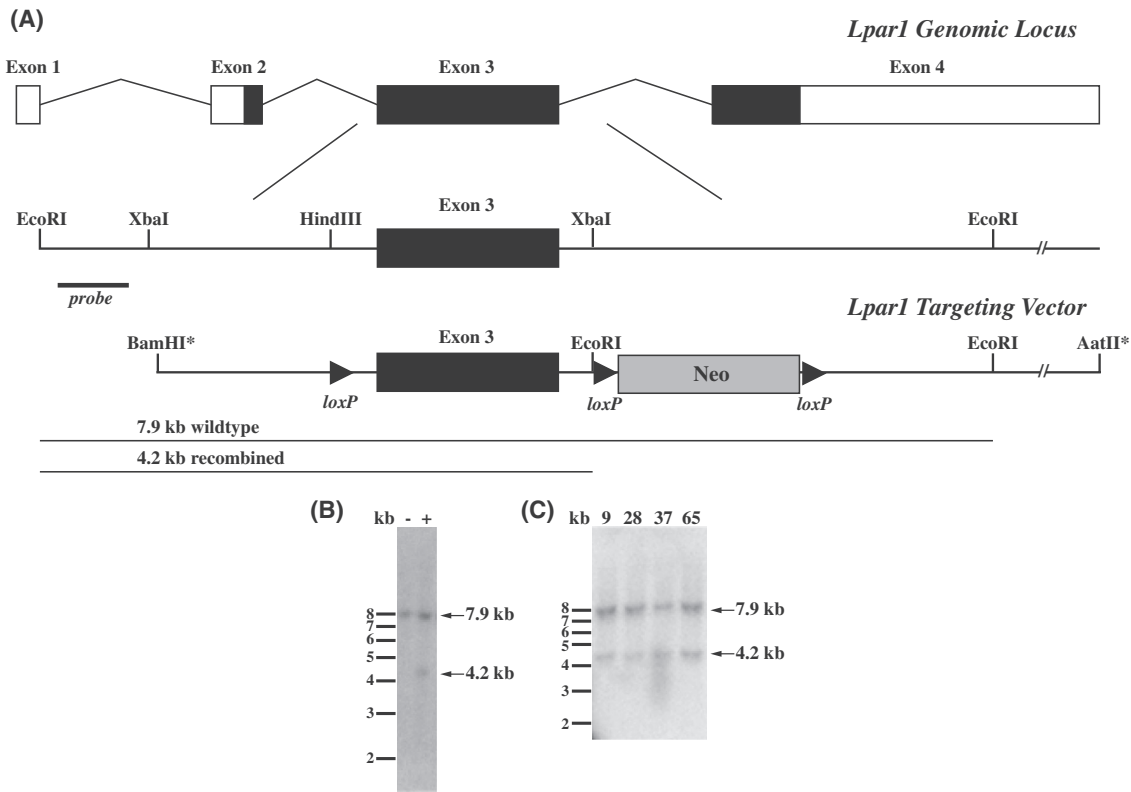


**FIGURE 1** Conditional gene targeting of the *Lpar1* gene locus and identification of ES cells positive for homologous recombination. A, Schematic of the *Lpar1* genomic locus, the region used for gene targeting, and the *Lpar1* targeting vector. In the targeting vector, loxP sites flank *Lpar1* exon 3 and the neomycin cassette used for ES cell drug resistance selection screening, an introduced EcoRI site allows for identification of homologous recombination events with the indicated external probe. Asterisks represent artificial restriction enzyme sites used in the construction of the targeting vector. B, Southern blot of EcoRI digested ES cell DNA hybridized with the radiolabeled probe shown in (A) identified an ES cell clone positive (+) for homologous recombination, as indicated by the presence of a 4.2 kb band. An ES cell clone with an incorrect recombination event (-) is shown for comparison and shows only the Wt 7.9 kb *Lpar1* band. C, Four identified ES cell clones (9, 28, 37, and 65) were grown and homologous recombination was reconfirmed by Southern blotting. These clones were chosen for loxP site retention screening, clones 37 and 65 were used for used for blastocyst injections.

a Bio-Rad Gene Pulser II (200 mVolts  $\times$  800  $\mu$ F capacitance). The electroporated ES cells were plated on mitotically inactive mouse feeder cells and allowed to recover for 24 hours at 37°C; 24 hours after electroporation and plating, 150  $\mu$ g/mL Geneticin (Invitrogen) was added to the ES cell medium and the cells were placed under selection for 7 days. ES cell clones were then isolated and grown individually for subsequent DNA isolation and screening for homologous recombination events by Southern blotting and hybridization with a *Lpar1* DNA probe containing sequence external to that of the 5' end of the *Lpar1* targeting vector. Clones with homologous recombination events were then screened for retention of the loxP site 5' to *Lpar1* exon 3 with the following primers: 5' loxP Forward 5'-gttgggacatggatgctattc-3' and 5' loxP Reverse 5'-aatctgttctcatcccacag-3'. Correctly targeted ES cell clones were then injected into C57BL/6J blastocysts at the TSRI Murine Genetics Core.

To delete the loxP flanked PGK-neo cassette in vivo, gene targeted mice were crossed to *nestin-cre* transgenic mice and resultant males were then bred to C57BL/6J female mice.

Male mice were chosen because cre is expressed in the germline of *nestin-cre* male mice. Offspring were then screened by PCR for the presence of the 5' loxP site with the primers listed above, for the presence or absence of the PGK-neo cassette with primers A1 Exon 3 Forward 5'-agactgtggcattgtgcttg-3' and Neo Reverse 5'-tggatgtggaatgtgtgcgag-3', and for retention of the loxP site 3' to *Lpar1* exon 3 with primers 3' loxP Forward 5'-tgcagaattatgagtggacagg-3' and 3' loxP Reverse 5'-ggtttagtgtgtggatcg-3'. Mice that retained the loxP sites 5' and 3' to *Lpar1* exon 3 but deleted the PGK-neo cassette were selected for propagation and crossing with *nestin-cre*, *P0-cre*, *synapsin-cre*, and *CD11b-cre* transgenic mice.<sup>32-35</sup>

PCR genotyping of the *Lpar1* conditional mutant mice was done with the following primers: 5' loxP Forward 5'-gttgggacatggatgctattc-3', 3' loxP Reverse 5'-ggtttagtgtgtggatcg-3', and A1 Exon 3 Forward 5'-agactgtggcattgtgcttg-3'. PCR amplification of genomic DNA with these primers identified Wt, *Lpar1*<sup>fllox</sup>, and *Lpar1* deleted products of 316, 354, and 242 bp, respectively. *Synapsin-cre*, *CD11b*, *P0-cre*, and *nestin-cre* transgenes were identified by PCR amplification

of genomic DNA with a common reverse PCR primer, (Cre Reverse 5'-CAG CAT TGC TGT CAC TTG GTC-3'), and forward primers specific for *synapsin* (SynCreForward 5'-CCCAAGAAGAAGAGGAAGGTG-3'), *CD11b* (CD11b Forward 5'-ACACCTCAGCCTGTCCAGTAG-3'), P0 (MPZ Forward (P0 Cre) 5'-ATT GGT CAC TGG CTC AAG AC-3'), and *nestin* (Nestin Prom: 5'-ACT CCC TTC TCT AGT GCT CCA-3') yielding products of 350 bp, 1 kb, 525 bp, and 550 bp, respectively.

## 2.4 | Southern blotting and DNA hybridization

ES cell clones were screened for homologous recombination by digesting 10 µg of ES cell DNA with EcoRI, running the DNA on a 0.8% 1 x TAE agarose gel, and transferring the digested DNA to Nytran SuPerCharge membrane (GE Healthcare Life Sciences) in 20 × SSPE. Transferred DNA was UV crosslinked to the membrane and hybridized with a <sup>32</sup>P-labeled (Prime-It II Random Primer Labeling Kit, Agilent) *Lpar1* probe with sequence external to the 5' end of the targeting vector. The 800 bp probe was produced by PCR from a BAC containing *Lpar1* with the following primers: A1 Ext Forward 5'-actgaggtcactactcagag-3' and A1 Ext Reverse 5'-gtctatgctgtggaattcaag-3'. Probe hybridization was carried out overnight at 42°C in a .05 M pH 7.4 phosphate buffer containing 50% formamide, 5 × SSPE, 1 × Denhart's, 1% SDS, containing .1% denatured 10 mg/mL salmon sperm DNA following a 1 hour pre-hybridization. Blots were washed and visualized using a phosphorimager. The presence of a 4.2 kb recombined band and a 7.9 kb Wt band was indicative of ES cells with homologous recombination events.

## 2.5 | Partial sciatic nerve ligation and behavioral testing

The partial sciatic nerve ligation (PSNL) procedure was performed as described.<sup>31</sup> Adult *Lpar1<sup>flox/flox</sup>* and *Lpar1<sup>flox/flox</sup>-cre* transgenic mice in a C57BL/6J background were anesthetized via nosecone delivery of isoflurane and the right limb sciatic nerve exposed and tightly ligated with 10-0 fine sutures. The wound and skin were closed and stitched, and the animals allowed to recover. For behavioral testing, animals were acclimated in cages with wire mesh bottoms for 1 hour prior to testing in an environmentally controlled testing room. Paw withdrawal threshold (gram (g)) against increasing mechanical stimuli (0-50 g in 20 seconds) were measured before and following PSNL surgery with tests conducted four separate times with at least a 1 minute interval between tests. The average response was normalized to pre-surgery controls ± SEM.

## 2.6 | Immunohistochemistry

DRG were isolated from the lumbar region of *Lpar1<sup>flox/flox</sup>* control and *Lpar1<sup>flox/flox</sup>*-conditional null-mutant mice. Tissues were embedded in OCT compound and 5 µM sections were cut and immunolabeled with antibodies to mouse LPA<sub>1</sub> (PA1 10401, Thermo Fisher Scientific) and MBP (ab134018, Abcam). Secondary antibodies were used against the listed primary antibodies and 60x images were acquired on a Zeiss Axio Imager.D2 microscope.

## 2.7 | Reverse transcription PCR

DRG were isolated from the lumbar region of *Lpar1<sup>flox/flox</sup>* and *Lpar1<sup>flox/flox</sup>-nestin-cre* conditional null-mutant mice. DRG were placed in 1 mL of TRIzol Reagent (Thermo Fisher Scientific) and total RNA was isolated according to the manufacturer's directions. cDNA was synthesized from total RNA using a Bio-Rad iScript cDNA synthesis kit and β-actin and *Lpar1*-specific oligonucleotide primer pairs were used to amplify target gene transcripts. Primers used to amplify a 350 bp product from β actin cDNA were M β Actin Forward 5'-tggaatcctgtggcatcatg-3' and M β Actin Reverse 5'-aaacgcagctcagtaacagtc-3'; primers used to amplify a 194 bp product from *Lpar1* cDNA were M LPA<sub>1</sub> Forward RT 5'-gacacatgatgagcctcttg-3' and M LPA<sub>1</sub> Reverse RT 5'-tcgeggtaggagtagatgatg-3'. An equivalent amount of cDNA from each sample was calibrated to produce equal amounts of β-actin PCR product to amplify the *Lpar1* cDNA.

## 3 | RESULTS

### 3.1 | Generation of *Lpar1* conditional null mutant mice

We selected a portion of the *Lpar1* genomic locus for conditional gene targeting in embryonic stem (ES) cells to create a mutant mouse (*Lpar1<sup>flox/flox</sup>*) where *Lpar1* exon 3 is selectively deleted in the presence of the cre recombinase (Figure 1A). The targeting vector contained a loxP site that was introduced into a restriction enzyme site 5' of exon 3, and a neomycin drug selection cassette flanked by loxP sites in a restriction enzyme site 3' of exon 3. Following electroporation of the linearized *Lpar1* targeting construct, drug selection, and screening of DNA isolated from selected ES cell clones by Southern blotting and hybridization, several clones with a homologously recombined *Lpar1* allele were identified (Figure 1B,C). PCR with primers flanking the 5' loxP site was used to select ES cell clones for blastocyst injection. Mice positive for germline transmission of the recombined allele were then crossed with *nestin-cre* transgenic mice to produce *Lpar1<sup>flox/flox</sup>-nestin-cre*

mice.<sup>34</sup> Because *nestin* is expressed in the testis, male *Lpar1<sup>flox</sup>/flox*-*nestin-cre* mice were bred to C57BL/6J female mice to produce offspring with germline *cre*-mediated loxP site recombination. Selective deletion of the floxed neomycin cassette and retention of the 5' loxP site in offspring were identified by PCR (Figure 2A,B). Heterozygous *Lpar1<sup>flox/+</sup>* mice with the correct recombination events were then crossed together to produce Wt, *Lpar1<sup>flox/+</sup>*, and *Lpar1<sup>flox/flox</sup>* mice (Figure 2C). A high level of embryonic lethality was observed for *Lpar1* constitutive null mutant mice in a C57BL/6J background, whereas *Lpar1<sup>flox/flox</sup>* mice in this background strain were healthy and indistinguishable from Wt littermates. Wt, *Lpar1<sup>flox/+</sup>*, and *Lpar1<sup>flox/flox</sup>* mice were differentiated by PCR (Figure 2C) and are behaviorally the same.

### 3.2 | Cre-mediated *Lpar1* targeted deletion

To delete *Lpar1* in all neural cell types, neurons, Schwann cells, and myeloid lineage cells, *Lpar1<sup>flox/flox</sup>* mice were crossed to *nestin*, *synapsin*, *P0*, and *CD11b-cre* transgenic mice, respectively.<sup>32-35</sup> To confirm that *Lpar1* was deleted in the presence of *cre*, genomic DNA was isolated from DRG of *Lpar1<sup>flox/flox</sup>* and *Lpar1<sup>flox/flox</sup>-nestin-cre* mice and PCR was used to verify genomic recombination of the *Lpar1* genomic locus to produce a null allele (Figure 3A). DRG contain both neural and nonneural cells, with conditional deletion limited

to neural cells, thus producing a recombined (neural) and unrecombined (nonneural) signal in conditional mutants. As expected, PCR products indicative of both an unrecombined and recombined *Lpar1<sup>flox/flox</sup>* allele can be amplified from genomic DNA isolated from *Lpar1<sup>flox/flox</sup>-nestin-cre* DRG, while only an unrecombined product can be produced from the DRG of control *Lpar1<sup>flox/flox</sup>* mice (Figure 3A). In agreement with genomic deletion of *Lpar1*, RT-PCR showed *Lpar1* mRNA transcripts are absent in *Lpar1<sup>flox/flox</sup>-nestin-cre* DRG (Figure 3B). Following Schwann cell-specific *P0-cre* crossing, PCR analyses of sciatic nerve showed deletion of *Lpar1* (Figure 3C) compared to Wt. Neuronal deletion was confirmed in the cerebral cortex (Ctx) of *Lpar1<sup>flox/flox</sup>-synapsin-cre* mice (Figure 3D). Immunofluorescent labeling of peripheral myelinated axons for myelin basic protein (MBP, red) and satellite glia expressing LPA<sub>1</sub> (green) in Wt DRG (Figure 3E) was not observed in *Lpar1<sup>flox/flox</sup>-nestin-cre* mice (Figure 3F). These data demonstrate conditional deletion of *Lpar1* in the presence of targeted *cre* recombinase expression.

### 3.3 | *Lpar1* expressing neural cell types contribute to PSNL-induced neuropathic pain phenotypes

To determine which *Lpar1* expressing neural cell types mediate PSNL-induced neuropathic pain protection, paw

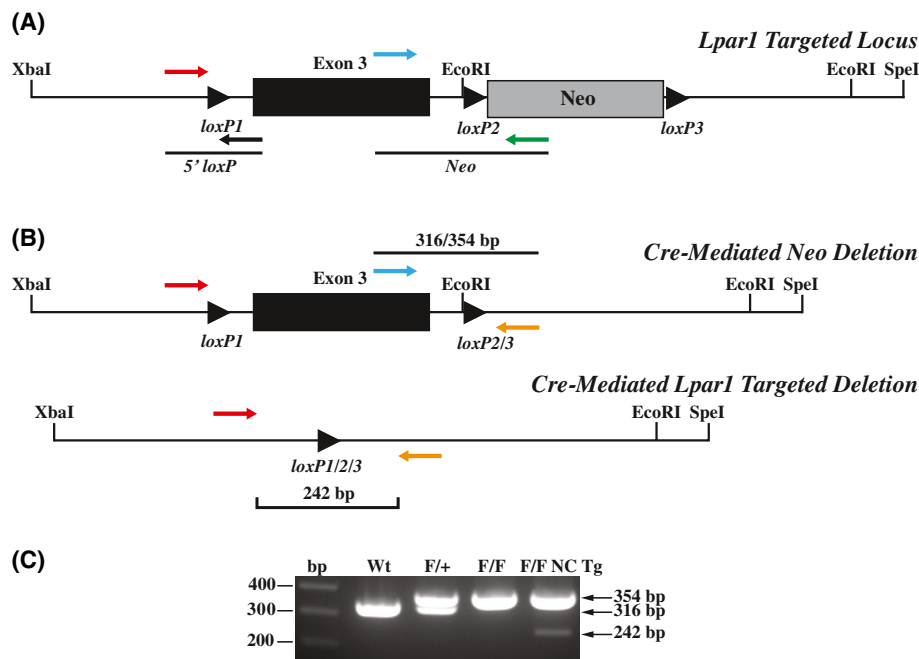


**FIGURE 2** Cre-mediated deletion in mice with a recombined *Lpar1* allele. A, Schematic showing PCR primer pairs used to screen for cre-mediated deletion of the floxed neomycin cassette. The primers shown assay for the presence of the 5' loxP site and the presence or absence of the neomycin cassette. B, Diagrams showing the finished *Lpar1* targeted allele produced through in vivo cre-mediated deletion of the neomycin cassette (top) and cre-mediated targeted deletion of floxed *Lpar1* exon 3 (bottom). The three-primer combination used for PCR genotyping is indicated. C, PCR genotyping of tail DNA from wildtype (Wt), *Lpar1<sup>flox/+</sup>* (F/+), *Lpar1<sup>flox/flox</sup>* (F/F), and *Lpar1<sup>flox/flox</sup>-nestin-cre* transgenic (F/F NC Tg) mice. Primers shown in (B) were used for PCR. Wt *Lpar1* produced bands of 316 bp, while floxed alleles produced bands 354 bp. The presence of a 242 bp band in the *Lpar1<sup>flox/flox</sup>-nestin-cre* sample is indicative of cre-mediated deletion in neural tissue present in the mouse tail.

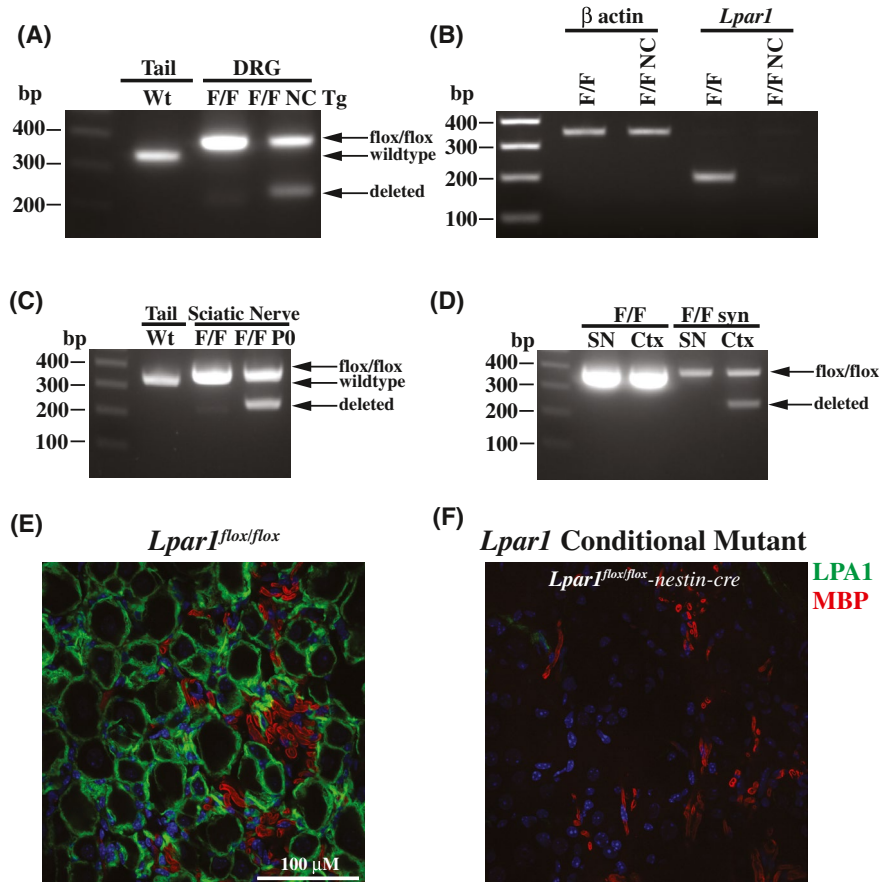


**FIGURE 3** Functional deletion of *Lpar1* is cre-dependent. A, PCR products of DNA isolated from *Lpar1*<sup>flox/flox</sup> (F/F) and *Lpar1*<sup>flox/flox</sup>-*nestin-cre* transgenic (F/F NC Tg) DRG shows genomic deletion of *Lpar1* exon 3 DNA from the tail of a Wt mouse is shown for comparison. B, qPCR products of cDNA prepared from *Lpar1*<sup>flox/flox</sup> (F/F) and *Lpar1*<sup>flox/flox</sup>-*nestin-cre* transgenic (F/F NC Tg) DRG shows that *Lpar1* transcripts are lost in neural tissues. C, PCR of genomic DNA isolated from the tail of a Wt mouse (Wt) and the sciatic nerve of *Lpar1*<sup>flox/flox</sup> (F/F) and *Lpar1*<sup>flox/flox</sup>-*P0-cre* (F/F P0) mice. D, PCR amplification of genomic DNA isolated from the sciatic nerve (SN) and cortex (Ctx) of *Lpar1*<sup>flox/flox</sup> and *Lpar1*<sup>flox/flox</sup>-*synapsin-cre* mice. The PCR primers used for amplification of Wt (316 bp), *Lpar1* floxed alleles (354 bp), and *Lpar1* deleted products (242 bp) are identical to those used in Figure 2B. The 100, 200, 300, and 400 bp bands of the 1kb plus DNA ladder are indicated for reference. E and F, Immunofluorescent labeling of peripheral myelinated axons identify Wt LPA<sub>1</sub> immunolabeling in *Lpar1*<sup>flox/flox</sup> mice (E) and its absence (F) in *Lpar1*<sup>flox/flox</sup>-*nestin-cre* transgenic mice. LPA<sub>1</sub> labeling is in green and MBP (myelin) in red for individual samples. Scale bar = 100 μM.

withdrawal threshold responses following cre recombination for *Lpar1*<sup>flox/flox</sup>-*nestin*, *Lpar1*<sup>flox/flox</sup>-*synapsin*, *Lpar1*<sup>flox/flox</sup>-*P0*, and *Lpar1*<sup>flox/flox</sup>-*CD11b-cre* were assessed. A rescued pain phenotype was observed for all genotypes compared to controls (Figure 4A-D). *Lpar1*<sup>flox/flox</sup>-*nestin-cre* conditional mutant mice challenged with PSNL had similar paw withdrawal threshold responses compared to previously defined *Lpar1* constitutive null mutant mice<sup>25</sup> (Figure 4A). By contrast, *Lpar1*<sup>flox/flox</sup>-*P0-cre* mice initially responded like control mice at early time points (Figure 4B; days 3 and 6), but then showed sustained protection at later time points (Figure 4E; day 9 through day 21). *Lpar1*<sup>flox/flox</sup>-*synapsin-cre* mice were initially refractory to PSNL-induced neuropathic pain (Figure 4C) but lost protection over time (Figure 4E; day 12 through day 21). Pain rescue was observed in *Lpar1*<sup>flox/flox</sup>-*CD11b-cre* mice compared to *Lpar1*<sup>flox/flox</sup> controls, with statistically significant protection observed at day 9 post-PSNL

(Figure 4D). It is notable that the combined protection of *P0* and *synapsin-cre* recombination approximated the protection produced by *nestin-cre* recombination (Figure 4A), implicating an additive rescue effect produced by both Schwann cells and neuronal LPA<sub>1</sub> activation in PSNL-initiated pain.

## 4 | DISCUSSION

*Lpar1* conditional null mutant mice were generated and shown to undergo cre-mediated recombination, enabling identification of *Lpar1*-expressing neurons and Schwann cells as functionally important for the PSNL phenotype. In the absence of cre, *Lpar1*<sup>flox/flox</sup> mice developed a pain phenotype comparable to Wt control mice,<sup>25</sup> demonstrating that this new floxed mutant gene functions normally in mice subject to PSNL. *Lpar1*<sup>flox/flox</sup>-*nestin-cre* mice with a

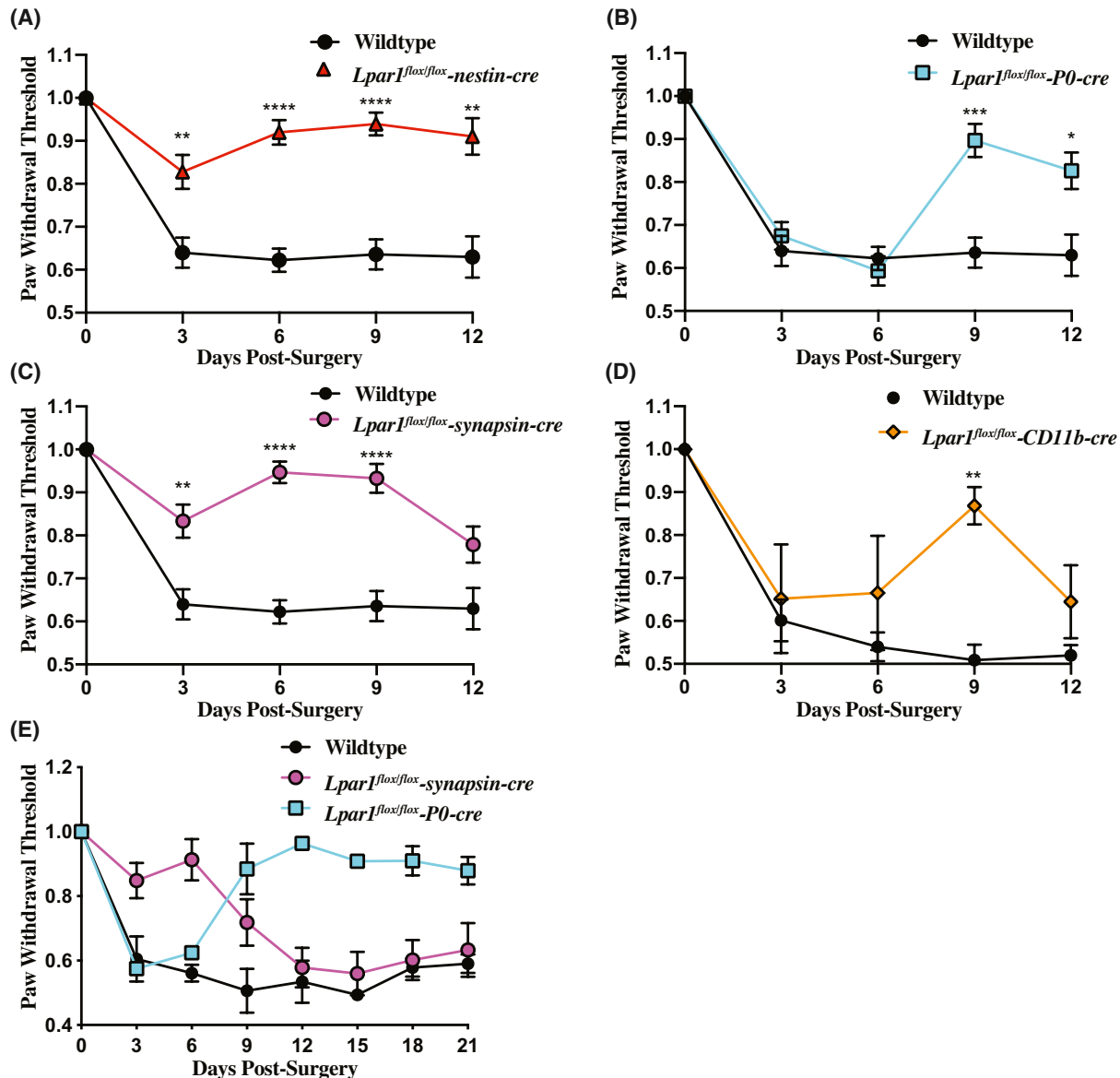


**FIGURE 4** Deletion of *Lpar1* in neuronal lineages protects against PSNL induced neuropathic pain. A, Targeted *nestin-cre*-mediated deletion of *Lpar1* in all neural lineages protects against neuropathic pain in the PSNL mouse model. B, Schwann cell-specific deletion of *Lpar1* through a *P0-cre* transgene protects mice from PSNL at later, but not earlier, time points. C, Specific deletion of *Lpar1* in neurons protects mice from PSNL induced neuropathic pain only at early time points. D, Deletion of *Lpar1* in CD11b expressing cell types provides protection from neuropathic pain at day 9 post-PSNL. E, Schwann cell-specific deletion of *Lpar1* occurs at later time points and is long-lasting. The plotted data are the average paw withdrawal threshold time observed for *Lpar1* conditional null mutants normalized to *Lpar1*<sup>flox/flox</sup> control animal responses  $\pm$  SEM. For (A, B, and C),  $N = 10$  *Lpar1*<sup>flox/flox</sup>,  $N = 10$  *Lpar1*<sup>flox/flox-nestin-cre</sup>,  $N = 9$  *Lpar1*<sup>flox/flox-P0-cre</sup>, and  $N = 8$  *Lpar1*<sup>flox/flox-synapsin-cre</sup> animals. For (D),  $N = 4$  *Lpar1*<sup>flox/flox</sup>, and  $N = 4$  *Lpar1*<sup>flox/flox-CD11b-cre</sup>. For (E),  $N = 2$  for all genotypes used. Statistical analysis was performed using a two-way ANOVA followed by a Sidak's multiple comparisons test and differences were considered significant when  $P \leq .05$  (\*= $P \leq .05$ , \*\* $\leq .001$ , \*\*\* $\leq .001$ , \*\*\*\* $P \leq .0001$ )

pan-neural lineage deletion of *Lpar1* were protected from PSNL-induced neuropathic pain which supports neural LPA<sub>1</sub> signaling as important despite *Lpar1*'s ubiquitous tissue expression. By comparison, *P0* and *synapsin-cre* recombination produced only partial rescue with complementary temporal phases of protection that appeared additive to account for the degree of rescue by *nestin-cre* recombination. Rescue from neuropathic pain was only

observed at day 9 in *Lpar1*<sup>flox/flox-CD11b-cre</sup> mice. It was recently reported that microglial depletion protects mice from PSNL-induced thermal hyperalgesia, therefore, we cannot exclude the possibility that CD11b expressing myeloid lineage cells also play a role in PSNL-induced neuropathic pain.<sup>36</sup>

The actions of LPA<sub>1</sub> in Schwann cells affecting PSNL phenotypes have not, to our knowledge, been previously

reported, and the observed phenotype was unexpected with regard to the clear and differential time-dependence of the effect. Explanations for these temporal changes in pain protection may be due to differences in de novo synthesis of LPA and the varied activation states documented for LPA<sub>1</sub><sup>8,11,37-40</sup> that may occur in neurons and Schwann cells. Such LPA signaling effects could be altered by receptor removal to produce the time-course differences observed for PSNL-initiated pain rescue. Long-lasting protection from neuropathic pain at later time points may also reflect changes in nerve myelination that may interfere with the transmission of pain stimuli as previously suggested.<sup>14,25</sup> Nerve fibers in *Lpar1<sup>flox/flox</sup>-PO-cre* mice may be abnormally myelinated, and nerve injury-induced demyelination may alter normal pain signal transmission. However, we note that the nerve fibers that respond to noxious stimuli are lightly myelinated A $\delta$  fibers and unmyelinated C-fibers,<sup>2,3</sup> requiring a more complex scenario that might involve central pain consolidation through myelinated fibers.

Effects of *Lpar1* deletion from neurons in *Lpar1<sup>flox/flox</sup>-synapsin-cre* mice showed early protection in PSNL, contrasting with later protection of Schwann cell receptor deletion, while supporting the involvement of neurons in LPA<sub>1</sub>-mediated PSNL-induced pain. *Synapsin-cre* deletion is effective in CNS neurons<sup>41</sup> but can be less effective in peripheral (DRG) neurons,<sup>33,42</sup> implicating central neuronal mechanisms. A possible explanation for rescue at early timepoints could involve a lack of de novo LPA synthesis from *Lpar1* deficient neurons. LPA can be released by neurons following nerve transection and neurons can synthesize LPA de novo through an LPA receptor dependent feed-forward mechanism (as evidenced by LPA<sub>3</sub>).<sup>15,26,43</sup> De novo LPA synthesis from other cell types following PSNL may result in LPA accumulation to drive neuropathic pain at later time points, particularly through activation of Schwann cell receptors in the neuron-specific mutants. Alternatively, PSNL may cause damage and vascular leakage that exposes peripheral nerves to LPA by activating cognate receptors to produce aberrant pain signaling.<sup>9,44-46</sup>

Other LPA receptor subtypes can contribute in distinct ways to neuropathic pain based on analyses of different LPA receptor-null mutants.<sup>13,16,25,31,39,47,48</sup> *Lpar5* null mutant mice are also protected from PSNL-induced neuropathic pain and show decreased sensitivity to acute pain stimuli and faster recovery responses when challenged in an inflammatory pain model.<sup>31,49</sup> Additionally, deletion of *Lpar3* in mice prevents i.t. LPA-induced de novo production of LPA in the dorsal horn and dorsal root and also prevents LPA-induced allodynia and hyperalgesia,<sup>26</sup> suggesting an LPA<sub>3</sub> mediated feed-forward mechanism for LPA in neuropathic pain initiation.<sup>27</sup> Prevention of LPA de novo synthesis and neuropathic pain in the i.t. LPA and PSNL neuropathic pain models using minocycline combined with *Lpar3* expression

in microglia indicate that this feed-forward mechanism is likely mediated by microglia.<sup>50,51</sup> In the present study, we observed a rescue effect of *Lpar1* loss from microglia only at day 9 post-PSNL, suggesting that maintained LPA<sub>3</sub> could sustain PSNL-initiated pain, and the possible involvement of *Lpar1* expressing CD11b expressing myeloid cell-types. *Cx3cr1<sup>CreER</sup>* transgenic mice that express the cre recombinase fused to a mutant estrogen ligand-binding domain, would be useful in delineating the contribution of microglia vs other CD11b expressing cell types in PSNL,<sup>52</sup> which could be pursued in the future.

The generated *Lpar1* conditional mutant mice will be useful in identifying other cell types involved in LPA<sub>1</sub> signaling in neuropathic pain models, as recently described for astrocytes,<sup>36</sup> as well as many other conditions and disease models.<sup>6-12,39,47,53,54</sup> The tractability of LPA<sub>1</sub> as a member of the lysophospholipid receptor family supports its potential as a druggable GPCR<sup>8,10,37,38</sup> and the development of novel therapies that target LPA<sub>1</sub>.

## ACKNOWLEDGMENTS

We thank Dr Andras Nagy for the R1 ES cells used for gene targeting, Grace Kennedy for histology expertise, Dr Gwendolyn Kaeser for statistical analysis, and Dr Gwendolyn Kaeser and Danielle Jones for editorial assistance. Funding was provided by the NIMH of the National Institutes of Health under award number R01MH051699 to JC and non-Federal funds from a predoctoral fellowship from Amira Pharmaceuticals to ML. The content is solely the responsibility of the authors and does not necessarily represent the official views of the National Institutes of Health.

## CONFLICT OF INTEREST

The authors declare no conflicts of interest with the contents of this article.

## AUTHOR CONTRIBUTIONS

R. Rivera, M. Lin, and J. Chun designed research; R. Rivera, M. Lin, and E. Bornhop performed research; R. Rivera created new conditional knockout mice; R. Rivera and M. Lin analyzed data; R. Rivera and J. Chun wrote the paper.

## REFERENCES

- van Hecke O, Austin SK, Khan RA, Smith BH, Torrance N. Neuropathic pain in the general population: a systematic review of epidemiological studies. *Pain*. 2014;155:654-662.
- D'Mello R, Dickenson AH. Spinal cord mechanisms of pain. *Br J Anaesth*. 2008;101:8-16.
- Dubin AE, Patapoutian A. Nociceptors: the sensors of the pain pathway. *J Clin Invest*. 2010;120:3760-3772.
- Ueda H. Molecular mechanisms of neuropathic pain-phenotypic switch and initiation mechanisms. *Pharmacol Ther*. 2006;109:57-77.

5. Latremoliere A, Woolf CJ. Central sensitization: a generator of pain hypersensitivity by central neural plasticity. *J Pain*. 2009;10:895-926.
6. Kihara Y, Maceyka M, Spiegel S, Chun J. Lysophospholipid receptor nomenclature review: IUPHAR Review 8. *Br J Pharmacol*. 2014;171:3575-3594.
7. Yung YC, Stoddard NC, Chun J. LPA receptor signaling: pharmacology, physiology, and pathophysiology. *J Lipid Res*. 2014;55:1192-1214.
8. Blaho VA, Chun J. "Crystal" clear? Lysophospholipid receptor structure insights and controversies. *Trends Pharmacol Sci*. 2018;39:953-966.
9. Choi JW, Herr DR, Noguchi K, et al. LPA receptors: subtypes and biological actions. *Annu Rev Pharmacol Toxicol*. 2010;50:157-186.
10. Kihara Y, Mizuno H, Chun J. Lysophospholipid receptors in drug discovery. *Exp Cell Res*. 2015;333:171-177.
11. Yung YC, Stoddard NC, Mirendil H, Chun J. Lysophosphatidic acid signaling in the nervous system. *Neuron*. 2015;85:669-682.
12. Chun J, Hla T, Moolenaar W, Spiegel S, eds. *Lysophospholipid Receptors : Signaling and Biochemistry*. Hoboken, NJ: Wiley; 2014.
13. Yang AH, Ishii I, Chun J. In vivo roles of lysophospholipid receptors revealed by gene targeting studies in mice. *Biochim Biophys Acta*. 2002;1582:197-203.
14. Anliker B, Choi JW, Lin ME, et al. Lysophosphatidic acid (LPA) and its receptor, LPA1, influence embryonic schwann cell migration, myelination, and cell-to-axon segregation. *Glia*. 2013;61:2009-2022.
15. Weiner JA, Fukushima N, Contos JJ, Scherer SS, Chun J. Regulation of Schwann cell morphology and adhesion by receptor-mediated lysophosphatidic acid signaling. *J Neurosci*. 2001;21:7069-7078.
16. Contos JJ, Fukushima N, Weiner JA, Kaushal D, Chun J. Requirement for the lpA1 lysophosphatidic acid receptor gene in normal suckling behavior. *Proc Natl Acad Sci U S A*. 2000;97:13384-13389.
17. Dubin AE, Herr DR, Chun J. Diversity of lysophosphatidic acid receptor-mediated intracellular calcium signaling in early cortical neurogenesis. *J Neurosci*. 2010;30:7300-7309.
18. Fincher J, Whiteneck C, Birgbauer E. G-protein-coupled receptor cell signaling pathways mediating embryonic chick retinal growth cone collapse induced by lysophosphatidic acid and sphingosine-1-phosphate. *Dev Neurosci*. 2014;36:443-453.
19. Fukushima N, Weiner JA, Kaushal D, et al. Lysophosphatidic acid influences the morphology and motility of young, postmitotic cortical neurons. *Mol Cell Neurosci*. 2002;20:271-282.
20. Hecht JH, Weiner JA, Post SR, Chun J. Ventricular zone gene-1 (vzq-1) encodes a lysophosphatidic acid receptor expressed in neurogenic regions of the developing cerebral cortex. *J Cell Biol*. 1996;135:1071-1083.
21. Suckau O, Gross I, Schrotter S, et al. LPA1, LPA2, LPA4, and LPA6 receptor expression during mouse brain development. *Dev Dyn*. 2019;248:375-395.
22. Estivill-Torres G, Llebreg-Zayas P, Matas-Rico E, et al. Absence of LPA1 signaling results in defective cortical development. *Cereb Cortex*. 2008;18:938-950.
23. Matas-Rico E, Garcia-Diaz B, Llebreg-Zayas P, et al. Deletion of lysophosphatidic acid receptor LPA1 reduces neurogenesis in the mouse dentate gyrus. *Mol Cell Neurosci*. 2008;39:342-355.
24. Harrison SM, Reavill C, Brown G, et al. LPA1 receptor-deficient mice have phenotypic changes observed in psychiatric disease. *Mol Cell Neurosci*. 2003;24:1170-1179.
25. Inoue M, Rashid MH, Fujita R, Contos JJ, Chun J, Ueda H. Initiation of neuropathic pain requires lysophosphatidic acid receptor signaling. *Nat Med*. 2004;10:712-718.
26. Ma L, Uchida H, Nagai J, et al. Lysophosphatidic acid-3 receptor-mediated feed-forward production of lysophosphatidic acid: an initiator of nerve injury-induced neuropathic pain. *Mol Pain*. 2009;5:64.
27. Ueda H. Lysophosphatidic acid signaling is the definitive mechanism underlying neuropathic pain. *Pain*. 2017;158(Suppl 1):S55-S65.
28. Ma L, Nagai J, Chun J, Ueda H. An LPA species (18:1 LPA) plays key roles in the self-amplification of spinal LPA production in the peripheral neuropathic pain model. *Mol Pain*. 2013;9:29.
29. Ma L, Uchida H, Nagai J, Inoue M, Aoki J, Ueda H. Evidence for de novo synthesis of lysophosphatidic acid in the spinal cord through phospholipase A2 and autotaxin in nerve injury-induced neuropathic pain. *J Pharmacol Exp Ther*. 2010;333:540-546.
30. Seltzer Z, Dubner R, Shir Y. A novel behavioral model of neuropathic pain disorders produced in rats by partial sciatic nerve injury. *Pain*. 1990;43:205-218.
31. Lin ME, Rivera RR, Chun J. Targeted deletion of LPA5 identifies novel roles for lysophosphatidic acid signaling in development of neuropathic pain. *J Biol Chem*. 2012;287:17608-17617.
32. Boillee S, Yamanaka K, Lobsiger CS, et al. Onset and progression in inherited ALS determined by motor neurons and microglia. *Science*. 2006;312:1389-1392.
33. Feltri ML, D'Antonio M, Previtali S, Fasolini M, Messing A, Wrabetz L. P0-Cre transgenic mice for inactivation of adhesion molecules in schwann cells. *Ann N Y Acad Sci*. 1999;883:116-123.
34. Tronche F, Kellendonk C, Kretz O, et al. Disruption of the glucocorticoid receptor gene in the nervous system results in reduced anxiety. *Nat Genet*. 1999;23:99-103.
35. Zhu Y, Romero MI, Ghosh P, et al. Ablation of NF1 function in neurons induces abnormal development of cerebral cortex and reactive gliosis in the brain. *Genes Dev*. 2001;15:859-876.
36. Ueda H, Neyama H, Nagai J, Matsushita Y, Tsukahara T, Tsukahara R. Involvement of lysophosphatidic acid-induced astrocyte activation underlying the maintenance of partial sciatic nerve injury-induced neuropathic pain. *Pain*. 2018;159:2170-2178.
37. Chrencik JE, Roth CB, Terakado M, et al. Crystal structure of antagonist bound human lysophosphatidic acid receptor 1. *Cell*. 2015;161:1633-1643.
38. Chun J, Kihara Y, Jonnalagadda D, Blaho VA. Fingolimod: lessons learned and new opportunities for treating multiple sclerosis and other disorders. *Annu Rev Pharmacol Toxicol*. 2019;59:149-170.
39. Lummis NC, Sanchez-Pavon P, Kennedy G, et al. LPA1/3 overactivation induces neonatal posthemorrhagic hydrocephalus through ependymal loss and ciliary dysfunction. *Sci Adv*. 2019;5:eaax2011.
40. Mirendil H, Thomas EA, De Loera C, Okada K, Inomata Y, Chun J. LPA signaling initiates schizophrenia-like brain and behavioral changes in a mouse model of prenatal brain hemorrhage. *Transl Psychiatry*. 2015;5:e541.
41. Choi JW, Gardell SE, Herr DR, et al. FTY720 (fingolimod) efficacy in an animal model of multiple sclerosis requires astrocyte sphingosine 1-phosphate receptor 1 (S1P1) modulation. *Proc Natl Acad Sci U S A*. 2011;108:751-756.

42. Feltri ML, Graus Porta D, Previtali SC, et al. Conditional disruption of beta 1 integrin in Schwann cells impedes interactions with axons. *J Cell Biol.* 2002;156:199-209.
43. Fukushima N, Weiner JA, Chun J. Lysophosphatidic acid (LPA) is a novel extracellular regulator of cortical neuroblast morphology. *Dev Biol.* 2000;228:6-18.
44. Eichholtz T, Jalink K, Fahrenfort I, Moolenaar WH. The bioactive phospholipid lysophosphatidic acid is released from activated platelets. *Biochem J.* 1993;291(Pt 3):677-680.
45. Schumacher KA, Classen HG, Spath M. Platelet aggregation evoked in vitro and in vivo by phosphatidic acids and lysoderivatives: identity with substances in aged serum (DAS). *Thromb Haemost.* 1979;42:631-640.
46. Lim TK, Shi XQ, Johnson JM, et al. Peripheral nerve injury induces persistent vascular dysfunction and endoneurial hypoxia, contributing to the genesis of neuropathic pain. *J Neurosci.* 2015;35:3346-3359.
47. Yung YC, Mutoh T, Lin ME, et al. Lysophosphatidic acid signaling may initiate fetal hydrocephalus. *Sci Transl Med.* 2011;3:99ra87.
48. Ye X, Hama K, Contos JJ, et al. LPA3-mediated lysophosphatidic acid signalling in embryo implantation and spacing. *Nature.* 2005;435:104-108.
49. Callaerts-Vegh Z, Leo S, Vermaercke B, Meert T, D'Hooge R. LPA5 receptor plays a role in pain sensitivity, emotional exploration and reversal learning. *Genes Brain Behav.* 2012;11:1009-1019.
50. Ma L, Nagai J, Ueda H. Microglial activation mediates de novo lysophosphatidic acid production in a model of neuropathic pain. *J Neurochem.* 2010;115:643-653.
51. Moller T, Contos JJ, Musante DB, Chun J, Ransom BR. Expression and function of lysophosphatidic acid receptors in cultured rodent microglial cells. *J Biol Chem.* 2001;276:25946-25952.
52. Goldmann T, Wieghofer P, Muller PF, et al. A new type of microglia gene targeting shows TAK1 to be pivotal in CNS autoimmune inflammation. *Nat Neurosci.* 2013;16:1618-1626.
53. Gennero I, Laurencin-Dalicieux S, Conte-Auriol F, et al. Absence of the lysophosphatidic acid receptor LPA1 results in abnormal bone development and decreased bone mass. *Bone.* 2011;49:395-403.
54. Tager AM, LaCamera P, Shea BS, et al. The lysophosphatidic acid receptor LPA1 links pulmonary fibrosis to lung injury by mediating fibroblast recruitment and vascular leak. *Nat Med.* 2008;14:45-54.

**How to cite this article:** Rivera RR, Lin M-E, Bornhop EC, Chun J. Conditional *Lpar1* gene targeting identifies cell types mediating neuropathic pain. *The FASEB Journal.* 2020;34:8833–8842. <https://doi.org/10.1096/fj.202000317R>